J Periodontal Implant Sci. 2019 Dec;49(6):366-381
https://doi.org/10.5051/jpis.2019.49.6.366
pISSN 2093-2278·eISSN 2093-2286

JPIS
Journal of Periodontal & Implant Science

Research Article
Implant Science

Check for updates

Bioactive characteristics of an implant surface coated with a pH buffering agent: an *in vitro* study

Hyung-Chul Pae [1], **Su-Kyoung Kim** [2], **Jin-Young Park** [1], **Young Woo Song** [1], **Jae-Kook Cha** [1], **Jeong-Won Paik** [1], **Seong-Ho Choi** [1,*]

[1]Department of Periodontology, Research Institute for Periodontal Regeneration, Yonsei University College of Dentistry, Seoul, Korea
[2]Implant R&D Center, Osstem Implant Co., Ltd., Busan, Korea

OPEN ACCESS

Received: Jul 22, 2019
Revised: Sep 15, 2019
Accepted: Oct 11, 2019

***Correspondence:**
Seong-Ho Choi
Department of Periodontology, Research Institute for Periodontal Regeneration, Yonsei University College of Dentistry, 50 Yonsei-ro, Seodaemun-gu, Seoul 03722, Korea.
E-mail: shchoi726@yuhs.ac
Tel: +82-2-22283185
Fax: +82-2-3920398

ORCID iDs
Hyung-Chul Pae
https://orcid.org/0000-0002-6365-3557
Jin-Young Park
https://orcid.org/0000-0002-6408-1618
Young Woo Song
https://orcid.org/0000-0003-1835-5646
Jae-Kook Cha
https://orcid.org/0000-0002-6906-7209
Jeong-Won Paik
https://orcid.org/0000-0002-5554-8503
Seong-Ho Choi
https://orcid.org/0000-0001-6704-6124

ABSTRACT

Purpose: The purpose of this study was to evaluate the effectiveness of conventional sandblasted, large-grit, acid-etched (SLA) surface coated with a pH buffering solution based on surface wettability, blood protein adhesion, osteoblast affinity, and platelet adhesion and activation.
Methods: Titanium discs and implants with conventional SLA surface (SA), SLA surface in an aqueous calcium chloride solution (CA), and SLA surface with a pH buffering agent (SOI) were prepared. The wetting velocity was measured by the number of threads wetted by blood over an interval of time. Serum albumin adsorption was tested using the bicinchoninic acid assay and by measuring fluorescence intensity. Osteoblast activity assays (osteoblast adhesion, proliferation, differentiation, mineralization, and migration) were also performed, and platelet adhesion and activation assays were conducted.
Results: In both the wetting velocity test and the serum albumin adsorption assay, the SOI surface displayed a significantly higher wetting velocity than the SA surface (P=0.000 and P=0.000, respectively). In the osteoblast adhesion, proliferation, differentiation, and mineralization tests, the mean values for SOI were all higher than those for SA and CA. On the osteoblast migration, platelet adhesion, and activation tests, SOI also showed significantly higher values than SA (P=0.040, P=0.000, and P=0.000, respectively).
Conclusions: SOI exhibited higher hydrophilicity and affinity for proteins, cells, and platelets than SA. Within the limits of this study, it may be concluded that coating an implant with a pH buffering agent can induce the attachment of platelets, proteins, and cells to the implant surface. Further studies should be conducted to directly compare SOI with other conventional surfaces with regard to its safety and effectiveness in clinical settings.

Keywords: Biocompatible coated materials; Dental implants; Immunoassay; Surface properties

INTRODUCTION

The use of titanium dental implants has improved with respect to rapid osseointegration and prosthetic loading, as well as an increased implant success rate. In particular, modifications to the surface of implants has played a major role in these improvements [1-6]. Topographical and chemical modifications of the implant surface have been shown to improve hydrophilicity and bone-implant contact [5,7-9]. Sandblasted, large-grit, acid-etched (SLA)

Author Contributions

Conceptualization: Su-Kyoung Kim; Formal analysis: Jin Young Park, Young Woo Song; Investigation: Su-Kyoung Kim; Methodology: Seong-Ho Choi; Project administration: Jae-Kook Cha, Seong-Ho Choi; Writing - original draft: Hyung Chul Pae; Writing - review & editing: Jin Young Park, Young Woo Song, Jae-Kook Cha, Jeong-Won Paik.

Conflict of Interest

Su-Kyoung Kim is a staff member and researcher at Osstem Implant Co., Ltd. and participated in the in vitro experiments and writing process. All other authors declare no conflict of interest associated with this study.

implant surfaces, which have both a microstructure and a macrostructure, have shown good clinical results in previous studies [1,2,4,7].

Furthermore, chemical modifications of SLA surfaces have been developed. SLActive (Straumann, Basel, Switzerland) consists of SLA implant surface that has been submerged in an isotonic sodium chloride solution to prevent carbon contamination from the atmosphere. According to a previous study, this surface is thought to promote early-stage bone formation [10]. A chemically activated, calcium-modified SLA surface has also been developed (Osstem Implant Co., Ltd., Busan, Korea); this surface is submerged in a calcium chloride solution instead of a sodium chloride solution. This calcium-modified surface showed similar bone-implant contact to that of the SLActive surface in a recent study using a rabbit model [11].

Interactions with blood cells and molecules on the implant surface could impact surface properties [12]. Proteins such as growth and differentiation factors are attracted to hydrophilic implant surfaces. In many studies, the biochemical characteristics of the implant surface, such as cell viability, proliferation, attachment, and differentiation, were tested through *in vitro* experiments using cells or cytokines, and these properties were found to influence cellular activities [12-14].

Formation of a sufficient fibrin clot offers a direct and stable link at the bone-to-implant interface; therefore, it plays an important role in thrombogenic responses and osseointegration [15]. When the fibrin clots on different implant surfaces were observed, a relationship was found between the implant surface and the extent of the fibrin clot [16].

In the process of drilling prior to implant placement, bone tissue undergoes trauma similar to a fracture. The site becomes relatively hypoxic, and the extracellular pH becomes acidic. In acidic conditions, the bone marrow stromal cells exhibit low alkaline phosphatase (ALP) activity and low collagen synthesis, 2 factors that are important in bone formation [17]. It has been reported that ALP activity decreased from a peak at a pH of 7.4 to almost zero below a pH of 7.0 [18]. Another study found that ALP activity and collagen synthesis, as well as glycolysis and DNA synthesis of osteoblasts, are also affected by acidic conditions [19]. In addition, platelet aggregation was also reduced by extracellular acidosis, as mediated by the calcium ion entry pathway [20].

The novel chemically activated SLA surface that is coated with a pH buffering solution was investigated. This surface is thought to display a high affinity for proteins, cells, and platelets, thereby promoting rapid and stable blood clotting and thrombogenesis. Therefore, the purpose of this study was to evaluate the effectiveness of an SLA surface coated with a pH buffering solution *in vitro* compared with a conventional SLA surface and a chemically activated calcium-modified SLA surface based on surface wettability, blood protein adhesion, osteoblast affinity, and platelet adhesion and activation.

MATERIALS AND METHODS

Preparation of titanium discs, implants, and reagents

Three types of titanium discs and implants were provided by Osstem Implant Co., Ltd.: 1) a conventional SLA surface (SA, serving as the negative control group), 2) a SLA surface in aqueous calcium chloride solution (CA, serving as the positive control group), and 3) a SLA

https://doi.org/10.5051/jpis.2019.49.6.366

JPIS
Journal of Periodontal & Implant Science

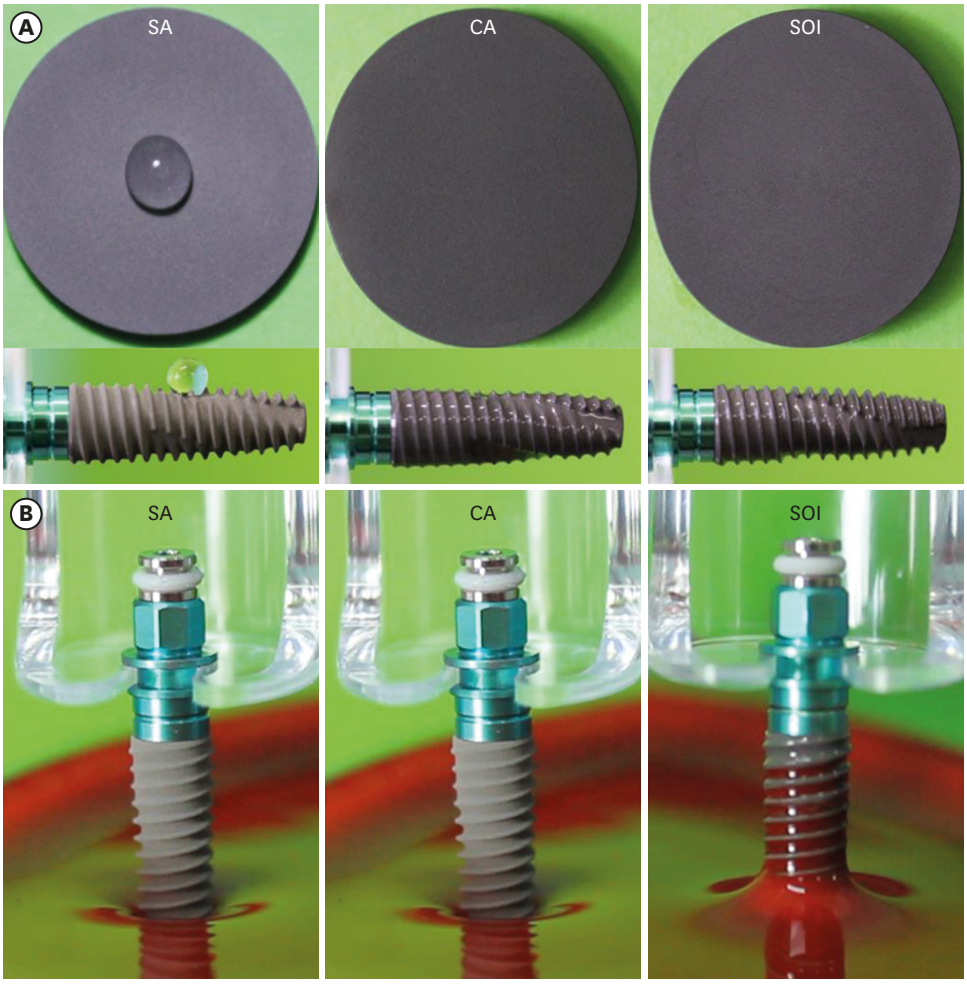

Figure 1. Surface wettability measurement. (A) Contact angle between a liquid drop and a solid surface. (B) Wetting velocity measurement. After 40 seconds, the SOI surface displayed the most threads wetted by blood. SA: conventional sandblasted, large-grit, acid-etched surface, CA: sandblasted, large-grit, acid-etched surface in aqueous calcium chloride solution, SOI: sandblasted, large-grit, acid-etched surface coated with pH buffering solution.

surface coated with a pH buffering solution (SOI, serving as the test group) (Figure 1A). The R_a values of the surfaces were 2.5±0.5 μm, based on information from the manufacturer. Cell culture plastic wares were purchased from Becton-Dickinson Falcon (Franklin Lakes, NJ, USA). Fetal bovine serum (FBS), trypsin/ethylenediaminetetraacetic acid (EDTA), penicillin and streptomycin, and Dulbecco's modified eagle medium (DMEM) were purchased from HyClone (Salt Lake City, UT, USA), and phosphate-buffered saline (PBS) was obtained from Invitrogen Corporation (Paisley, UK). Alizarin Red S, Triton X-100, *p*-nitrophenylphosphate (p-NPP), magnesium chloride, and cresyl violet were purchased from Sigma (St. Louis, MO, USA), and 3-(4,5-dimethylthiazol-2-gl)-5-(3-carboxymethoxylphenyl)-2-(4-sulfophenyl-2H)-tetrazolium inner salt (MTS) was obtained from Promega (Madison, WI, USA). Three discs of each titanium surface (SA, CA, and SOI) were utilized for each test.

Surface wettability measurement (wetting velocity measurement)

efibrinated sheep blood (MB-S1876; MB Cell, Seoul, Korea) was placed in a dish (diameter, 10 cm) to a depth of 2–3 cm. Implants with SA, CA, and SOI surfaces (diameter, 4.5 mm; length,

https://doi.org/10.5051/jpis.2019.49.6.366

13 mm) were immersed into the blood up to 2 mm from the apex (Figure 1B). Nine implants for each surface were tested. The number of threads wetted by blood in 40 seconds was counted for the calculation of the wetting velocity.

Serum albumin adsorption

Bicinchoninic acid assay

Purified bovine serum albumin (BSA, 1 mg/mL, 1 mL) was added to the surfaces of the titanium discs. After incubation at 37°C for 1 hour, the non-adsorbed plasma was washed out. The BSA-treated discs were eluted for 30 minutes using a lysis buffer (0.2% Triton X-100 in PBS, pH 7.4) at 37°C. The supernatants were assayed using comparative bicinchoninic acid (BCA) assays (BCA Protein Assay Kit No. 23227) according to instructions provided by the supplier (Pierce, Rockford, IL, USA). Protein detection was performed at a wavelength of 560 nm using a multimode microplate reader (DTX 880 Multimode Detector, Beckman Coulter GmbH, Krefeld, Germany). Nine titanium discs of each surface were tested.

Fluorescein isothiocyanate (FITC)-labeled BSA

FITC-labeled BSA (Sigma) in PBS was used for the protein adsorption test. Adsorption was measured using fluorescence intensity. FITC-conjugated serum albumin was added in order to examine plasma protein adsorption by the SA, CA, and SOI implants. After incubation, the excess FITC-conjugated serum albumin was washed from the implant surfaces. Three implants of each surface were treated with FITC-conjugated serum albumin, examined using a Typhoon FLA 7000 device (GE Healthcare Life Sciences, Chicago IL, USA), and analyzed using Image J software (National Institute of Health, Bethesda, MD, USA) (Figure 2).

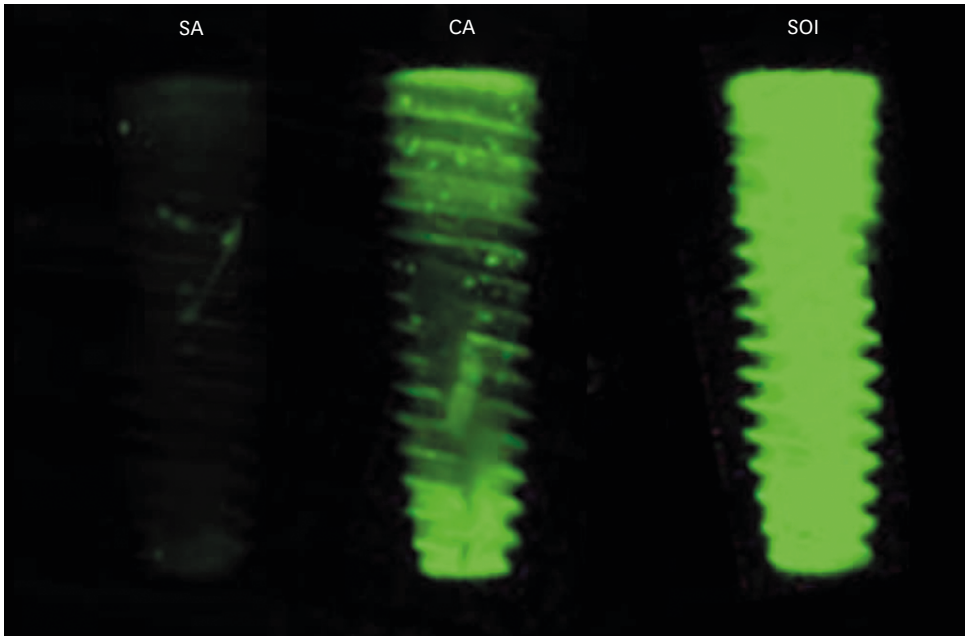

Figure 2. Image depicting FITC-labeled BSA present on each implant surface. The fluorescence intensity of the SOI surface was the strongest, whereas that of the SA surface was the weakest.
FITC: fluorescein isothiocyanate, BSA: bovine serum albumin, SA: conventional sandblasted, large-grit, acid-etched surface, CA: sandblasted, large-grit, acid-etched surface in aqueous calcium chloride solution, SOI: sandblasted, large-grit, acid-etched surface coated with pH buffering solution.

https://doi.org/10.5051/jpis.2019.49.6.366

Observation for osteoblast morphology

Cell culture (osteoblast culture)

The MG-63 cell line (ATCC, Manassas, VA, USA), established from human osteosarcoma cells, is a non-transformed cell line. These cells were routinely cultured in DMEM with 10% FBS and 0.1 mg/mL of penicillin and streptomycin. The cells were subcultured in trypsin/EDTA twice per week, and the medium was changed every 2 days.

Scanning electron microscopy (SEM)

For SEM observations, the MG-63 cells were incubated on the titanium discs and fixed with a 2.5% glutaraldehyde solution. After dehydration, the samples were sputter-coated with Pt-Pd for morphologic examination with SEM (JSM-6480LV, Tokyo, Japan) (Figure 3).

Confocal laser scanning microscopy (CLSM; immunofluorescence cell staining)

The cell morphology and cytoskeletal arrangement of osteoblasts were observed with CLSM. MG-63 cells were seeded for 24 hours on the titanium discs and observed using CLSM. The cells were fixed in 4% formalin and permeabilized in 0.1% Triton X-100. The cells were then blocked in 7.5% BSA containing PBS for 1 hour. The fluorescent staining was conducted with vinculin and F-actin using anti-vinculin Alexa Fluor 488 (Bioscience, Allentown, PA, USA) and anti-stain 555 fluorescent phalloidin (Cytoskeleton Inc., Denver, CO, USA), respectively. After incubation overnight at 4°C, the samples were then observed with CLSM (LSM 700, Carl Zeiss, Oberkochen, Germany) (Figure 4).

Osteoblast adhesion

With a CellTiter 96® AQ_{ueous} Non-Radioactive Cell Proliferation Assay kit (Promega), the cell adhesion assay of MG-63 cells was performed according to the manufacturer's instructions.

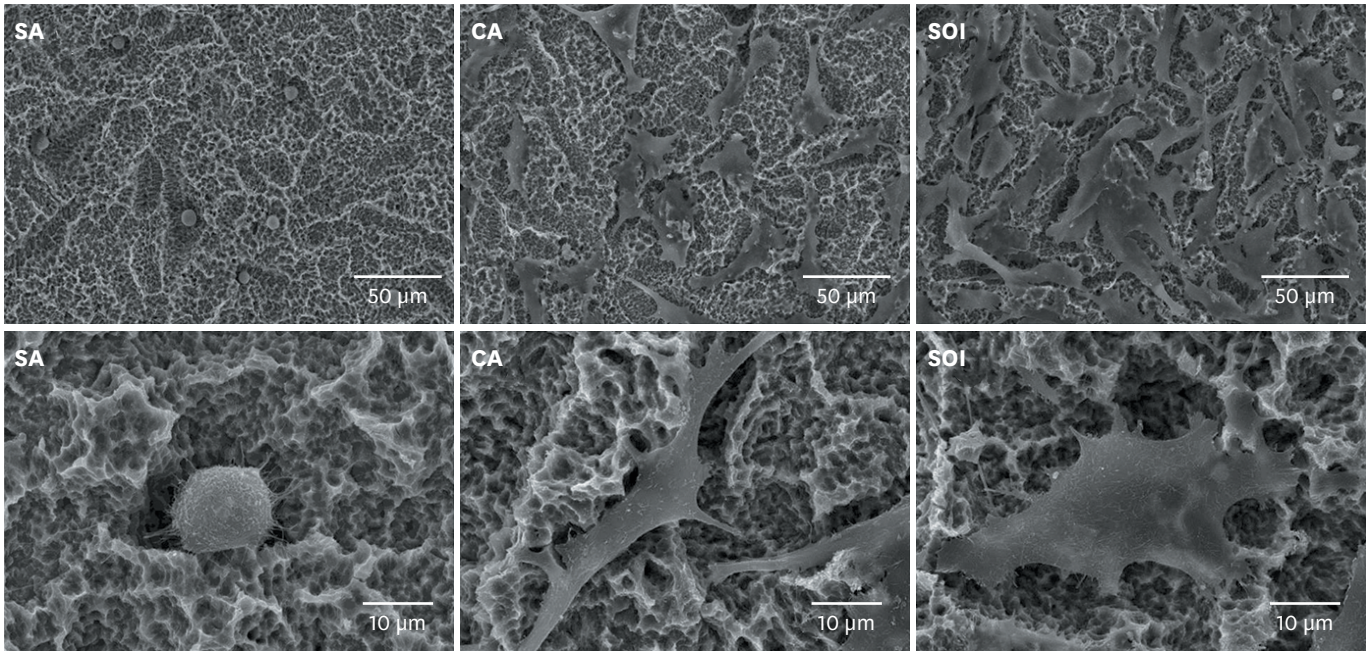

Figure 3. SEM image taken 30 minutes after MG-63 cell incubation on each implant surface. The number of osteoblasts on the CA and SOI surfaces is more prominent than that on the SA surface, and the cells on the CA and SOI surfaces seem to be further differentiated.
SA: conventional sandblasted, large-grit, acid-etched surface, CA: sandblasted, large-grit, acid-etched surface in calcium chloride aqueous solution, SOI: sandblasted, large-grit, acid-etched surface coated with pH buffering solution.

https://doi.org/10.5051/jpis.2019.49.6.366

JPIS
Journal of Periodontal & Implant Science

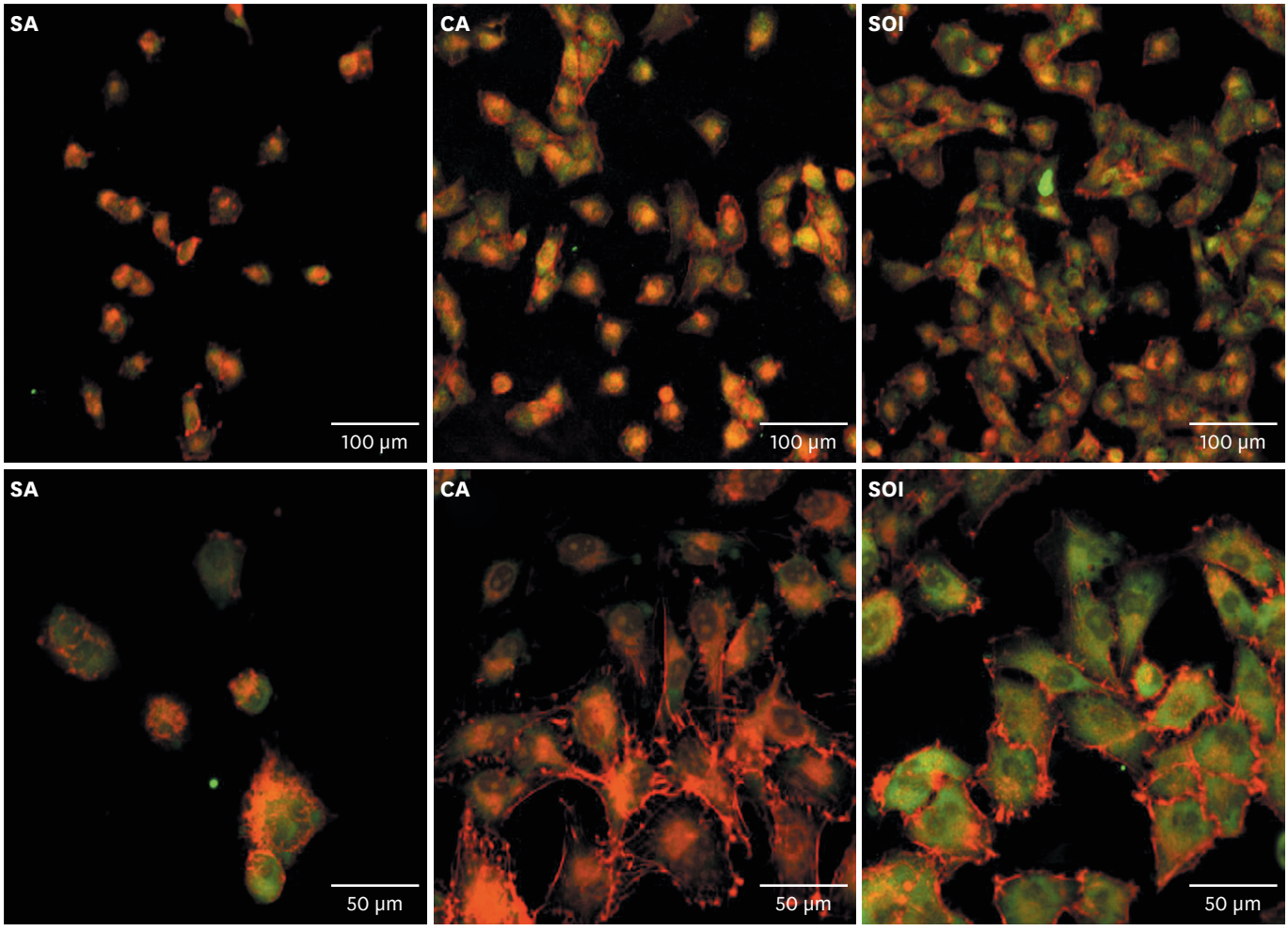

Figure 4. Confocal laser scanning microscopy (immunofluorescence cell staining) image taken 30 minutes after MG-63 cell incubation on each implant surface. Red indicates phalloidin staining, while green indicates vinculin staining. More bone cells were observed on the CA and SOI surfaces than on the SA surface. SA: conventional sandblasted, large-grit, acid-etched surface, CA: sandblasted, large-grit, acid-etched surface in calcium chloride aqueous solution, SOI: sandblasted, large-grit, acid-etched surface coated with pH buffering solution.

Prior to the cell adhesion assay, the cells were cultured onto either the titanium discs or the plastic material used for culture in 24 multi-well plates (Becton-Dickinson Falcon) at a density of 1×10^5 cells for 1 hour. Three titanium discs of each surface were tested. After the culture media was removed and washed, 500 μL of MTS/1-methoxy phenazine methosulfate (PMS)/medium mixture was added to each well for 2 hours. Colorimetric measurements of formazan dye were conducted using a DTX 880 device, and the optical density (OD) was read at 490 nm.

Osteoblast proliferation

Using a CellTiter 96® AQ_{ueous} Non-Radioactive Cell Proliferation Assay kit, the proliferation assay of MG-63 cells was performed according to the manufacturer's instructions. The cells were cultured onto either the titanium discs or the culture plastic. Three titanium discs of each surface were tested. After a period of time, the culture media was removed, and 500 μL of the MTS/PMS/medium mixture was combined into each well for 2 hours. Colorimetric measurements of formazan dye were conducted using a DTX 880 device, and the OD was read at 490 nm.

https://doi.org/10.5051/jpis.2019.49.6.366

Osteoblast differentiation (ALP activity)

ALP activity was examined as described in previous studies [21-24], with MG-63 cells cultured onto either the titanium discs or the culture plastic. Three titanium discs of each surface were tested. The osteogenic medium (containing 0.5 μM dexamethasone, 50 μg/mL L-ascorbic acid, and 10 mM β-glycerophosphate) [25,26] was replaced every 2 days. After a period of time, the cells were washed out and gathered in an ALP lysis buffer. The dissolved protein was extracted, and 100 g of protein was incubated with p-NPP using the ALP assay buffer in order to measure ALP activity in isolated cell supernatants. The degree of the colorimetric reaction was measured using a DTX 880 device to obtain an OD measurement at 405 nm.

Osteoblast mineralization (Alizarin Red S staining)

The experimental samples were stained with Alizarin Red S as reported elsewhere [27-29], with minor modifications. MG-63 cells were cultured on either the titanium discs or the culture plastic. Three titanium discs of each surface were tested. The osteogenic medium was replaced every 2 days. After a period of time, the cells were washed out and then fixed in 10% formaldehyde (Junsei, Tokyo, Japan). The cells were stained with 2% Alizarin Red S at a pH of 4.2 for 20 minutes. The stained cells were collected using the typical collection process. The absorbance level of Alizarin Red S was measured at 405 nm.

Osteoblast migration (chemotaxis assay: Transwell® cell migration assay)

For cell migration, MG63 cells (1×10^6 cells/mL) were suspended in a 0.1% BSA DMEM medium, and 350 μL of cell suspension was plated in the upper chambers of a Transwell® unit (8 μm pore size, SPL Insert; SPL Life Sciences, Pocheon, Korea) and incubated. The lower chambers were filled with 1 mL of the implant eluents. After 2 hours, the upper chambers were removed and the Transwell® insert was wiped with a cotton-tipped applicator. The inserts were stained with 0.2% cresyl violet, and the stained cells were eluted with citric acid. Colorimetric measurements of cresyl violet were performed using a DTX 880 device, and the OD was read at 590 nm. Nine titanium discs of each surface were tested.

Platelet adhesion

Platelet isolation (platelet-rich plasma)

Blood was obtained by cardiac puncture of a 2.5- to 3.0-kg New Zealand rabbit using a 21G needle into 4% sodium citrate (Fisher Scientific, Pittsburgh, PA, USA). Platelet-rich plasma (PRP) was made according to the technique described in a previous paper [30]. The PRP was incubated with calcium chloride (final concentration, 5 mM) (Fisher Scientific) at 37°C for 10 minutes.

Lactate dehydrogenase assay

The platelet solution had a concentration of 1×10^8 platelets/mL in PBS. To this solution, calcium chloride was added to yield a concentration of 2.5 mM, after which magnesium chloride was added to yield a final concentration of 1.0 mM. After 30 minutes at 37°C, the platelet suspension was placed on the titanium discs and left to adhere for 1 hour at 37°C. Nine titanium discs of each surface were tested. The platelet suspension was rinsed away to remove the non-adherent platelets. The platelet adhesion level was quantified by a lactate dehydrogenase (LDH) assay. LDH, which is released when the adherent platelets are lysed, was measured with a Triton-PBS buffer and a CytoTox 96® Non-Radioactive Cytotoxicity assay (Promega). The methods reported in previous studies [31,32] were used with modifications.

https://doi.org/10.5051/jpis.2019.49.6.366

SEM observation of the fibrin network

Preparation of the blood sample to obtain a fibrin clot

As previously described by Park and Davies [33], titanium discs were inserted so as to be almost press-fit into the bottoms of 24-well plates. One milliliter of PRP was added to each well and was gently mixed with blood proteins captured within the fibrin network at 37°C for 24 hours.

Preparation of the washed fibrin clot and SEM observation

To prepare for SEM observation, the fibrin clot samples were lightly rinsed with PBS and then fixed for 1 hour at room temperature using a special fixation buffer (2.5% glutaraldehyde dissolved in Dulbecco's PBS buffer at a pH of 7.0). After dehydrating the adherent fibrin network with an ethanol/water mixture, the samples were treated with hexamethyldisilazane (Sigma) and dried. The SEM procedure was completed by critical point drying of the material. The adherent fibrin networks were observed using SEM (Figure 5).

Platelet activation

Preparation of human platelet samples and incubation of titanium discs

PRP was obtained from 3 healthy volunteers in the manner previously described [34]. As outlined by Park and Davies [33], titanium discs were inserted so as to be almost press-fit into the bottoms of 24-well plates. Nine titanium discs of each surface were tested. One milliliter of PRP was added to each well. In order to stimulate interactions between the surfaces and the platelets, the plate was gently mixed at 37°C. The supernatant was pipetted off after 1 hour for further analysis.

Enzyme-linked immunoassay (ELISA) for P-selectin

As an index of platelet activation, P-selectin, a platelet membrane glycoprotein that is expressed when platelets are activated, was measured. The previously prepared supernatants were assayed using an ELISA to measure the concentration of soluble P-selectin. All assays were performed according to the manufacturer's instructions.

Statistical analysis

Statistical analysis was performed using SPSS version 23.0 (IBM Corp., Armonk, NY, USA). The records from each experiment were used to calculate the mean and standard deviation values of threads per second and the OD of the assays conducted on the 3 implant surfaces (SA, CA, and SOI). The Kruskal-Wallis test and the Mann-Whitney test (nonparametric analysis of variance) were used to analyze the differences among the 3 implant surfaces. A *P* value of less than 0.05 was considered to indicate statistical significance. For some tests with n<4, a statistical analysis could not be conducted, and only the mean and standard deviation were presented.

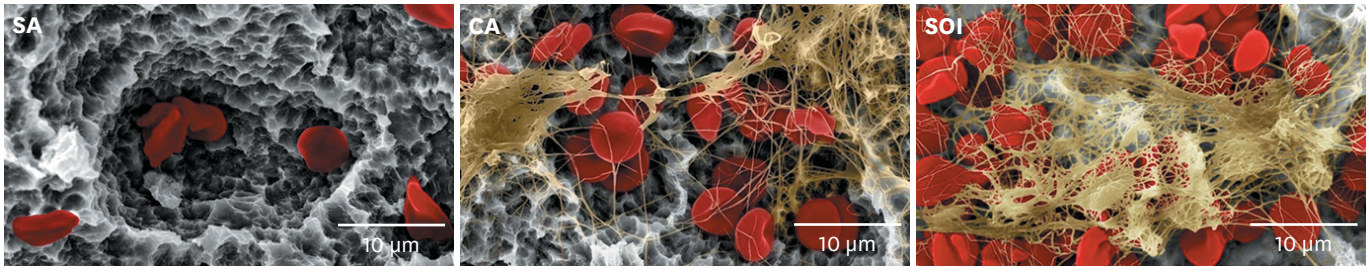

Figure 5. Scanning electron microscopy image of fibrin networks on each implant surface 1 hour after fibrin clot fixation. On the SOI surface, numerous red blood cells were visible, and the fibrin network was densely present above and around the red blood cells.
SA: conventional sandblasted, large-grit, acid-etched surface, CA: sandblasted, large-grit, acid-etched surface in calcium chloride aqueous solution, SOI: sandblasted, large-grit, acid-etched surface coated with pH buffering solution.

https://doi.org/10.5051/jpis.2019.49.6.366

JPIS Journal of Periodontal & Implant Science

RESULTS

Surface wettability measurements (wetting velocity measurements)

Implants with the SA, CA, and SOI surfaces were immersed in blood for the measurement of wetting velocity (Figure 1B). The mean wetting velocity for each implant surface was measured as 0.000 threads/second, 0.069 threads/second, and 0.124 threads/second, respectively (Table 1). The difference between the wetting velocities of the SA and CA surfaces was statistically significant (P=0.000). The differences between the wetting velocities of the SA and SOI surfaces and between those of the CA and SOI surfaces were also statistically significant (P=0.000 and P=0.000, respectively).

Serum albumin adsorption

BCA assay

Serum albumin was added to the titanium discs with the SA, CA, and SOI surfaces. The mean serum albumin adsorption for each surface was measured as 0.281, 1.120, and 1.287 OD, respectively (Table 2). The differences between serum albumin adsorption of the SA and CA surfaces were statistically significant (P=0.000). The differences between those of the SA and SOI surfaces and those of the CA and SOI surfaces were statistically significant (P=0.000 and P=0.000, respectively).

FITC-labeled BSA

The mean protein adsorption as measured by the fluorescence intensity for the SA, CA, and SOI surfaces was 3,972, 1,599,268, and 3,102,829 pixels, respectively. The data are reported in Table 2. A statistical analysis of the differences between the groups could not be conducted because of the lack of a sufficiently large sample size. Nevertheless, large differences in fluorescence intensity could be seen between the groups, with the SA surface displaying the lowest values and the SOI surface the highest.

Observation of osteoblast morphology

SEM

MG-63 cells were incubated on each of the SA, CA, and SOI surfaces. The number of osteoblasts on the CA and SOI surfaces was higher than that on the SA surface, and the cells of the CA and SOI surfaces seemed to be further differentiated. No prominent difference was

Table 1. Wetting velocity

Type of surface (n=9)	SA	CA	SOI
Velocity (threads/second)	0	0.069±0.005[a)]	0.124±0.012[a)]

Values are presented as mean±standard deviation.
SA: conventional sandblasted, large-grit, acid-etched surface, CA: sandblasted, large-grit, acid-etched surface in calcium chloride aqueous solution, SOI: sandblasted, large-grit, acid-etched surface coated with pH buffering solution.
[a)]Statistically significant difference compared to the SA group.

Table 2. Serum albumin adsorption

Type of surface	SA	CA	SOI
BSA (OD) (n=9)	0.281±0.006	1.120±0.024[a)]	1.287±0.040[a)]
FITC-labeled BSA (pixels) (n=3)	3,972±607	1,599,268±119,340	3,102,829±72,992

Values are presented as mean±standard deviation.
SA: conventional sandblasted, large-grit, acid-etched surface, CA: sandblasted, large-grit, acid-etched surface in calcium chloride aqueous solution; SOI: sandblasted, large-grit, acid-etched surface coated with pH buffering solution, OD: optical density, FITC: fluorescein isothiocyanate, BSA: bovine serum albumin.
[a)]Statistically significant difference compared to the SA group.

https://doi.org/10.5051/jpis.2019.49.6.366

observed between the CA and SOI surfaces, but the number of osteoblasts on the SOI surface was estimated to be slightly higher (Figure 3).

CLSM

MG-63 cells were incubated on each of the SA, CA, and SOI surfaces. Immunofluorescence staining was performed for vinculin and F-actin, which constitute the cytoskeleton of the cell. As in the SEM observations, more bone cells were observed on the CA and SOI surfaces than on the SA surface (Figure 4).

Osteoblast adhesion

The mean measurements of the cell adhesion assay for the SA, CA, and SOI surfaces were 0.438, 0.842, and 0.949 OD, respectively. The data are reported in Table 3. A statistical analysis of the differences between the groups could not be conducted because of the lack of a sufficiently large sample size; however, the SA surface showed the lowest value for the cell adhesion assay.

Osteoblast proliferation

The mean measurements of the cell proliferation assay for the SA, CA, and SOI surfaces were 0.701, 0.837, and 0.912 OD, respectively. The data are reported in Table 3. A statistical analysis of the differences between the groups could not be conducted because of the lack of a sufficiently large sample size; the SA surface showed the lowest value and the SOI surface showed the highest value, but overall, there seemed to be little difference between the groups.

Osteoblast differentiation

The mean measurements of the osteoblast differentiation assay for the SA, CA, and SOI surfaces were 0.350, 0.379, and 0.385 OD, respectively. The data are reported in Table 3. A statistical analysis of the differences between the groups could not be conducted because of the lack of a sufficiently large sample size; the SA surfaces showed the lowest value and the SOI surface showed the highest value, but overall, there seemed to be little difference between the groups.

Osteoblast mineralization

The mean measurements of the osteoblast mineralization assay for the SA, CA, and SOI surfaces were 320.4, 382.6, and 452.1 nM, respectively. The data are reported in Table 3. A statistical analysis of the differences between the groups could not be conducted because of the lack of a sufficiently large sample size; however, the SA surfaces seemed to show the lowest value for the cell adhesion assay.

Table 3. Osteoblast adhesion, proliferation, differentiation, mineralization, and migration

Type of surface	SA	CA	SOI
Adhesion (OD) (n=3)	0.438±0.015	0.842±0.028	0.949±0.038
Proliferation (OD) (n=3)	0.701±0.016	0.837±0.027	0.912±0.023
Differentiation (OD) (n=3)	0.350±0.010	0.379±0.005	0.385±0.005
Mineralization (nM) (n=3)	320.4±23.0	382.6±20.1	452.1±28.9
Migration (OD) (n=9)	0.195±0.013	0.195±0.012	0.215±0.018[a)]

Values are presented as mean±standard deviation.
SA: conventional sandblasted, large-grit, acid-etched surface, CA: sandblasted, large-grit, acid-etched surface in calcium chloride aqueous solution, SOI: sandblasted, large-grit, acid-etched surface coated with pH buffering solution, OD: optical density.
[a)]Statistically significant difference compared to the SA and CA groups.

https://doi.org/10.5051/jpis.2019.49.6.366

Table 4. Platelet adhesion and activation

Type of surface	SA	CA	SOI
Adhesion (OD) (n=9)	0.185±0.016	0.255±0.031[a)]	0.298±0.042[a,b)]
Activation (OD) (n=9)	0.112±0.014	0.251±0.024[a)]	0.414±0.046[a,b)]

Values are presented as mean±standard deviation.
SA: conventional sandblasted, large-grit, acid-etched surface, CA: sandblasted, large-grit, acid-etched surface in calcium chloride aqueous solution, SOI: sandblasted, large-grit, acid-etched surface coated with pH buffering solution, OD: optical density.
[a)]Statistically significant difference compared to the SA group; [b)]Statistically significant difference compared to the CA group.

Osteoblast migration

The mean measurements of soluble P-selectin ELISA for the SA, CA, and SOI surfaces were 0.195, 0.195, and 0.215 OD, respectively (Table 3). The difference between the SA and CA surface groups was not statistically significant (P=0.931). However, the SOI surface showed a statistically significantly higher value than either the SA or the CA group (P=0.040 and P=0.031, respectively).

Platelet adhesion

The mean measurements of the LDH assay for platelet adhesion to the SA, CA, and SOI surfaces were 0.185, 0.255, and 0.298 OD, respectively (Table 4). The difference in the LDH assay between the SA and CA surfaces was statistically significant (P=0.000). In addition, the SOI surface showed a statistically significantly higher value than both the SA and the CA groups (P=0.000 and P=0.040, respectively).

SEM observation of the fibrin network

The morphology of the fibrin networks adherent to each surface was observed. On the SA implant surfaces, the fewest red blood cells were visible, and a fibrin network was hardly observed. In contrast, a large number of red blood cells were located on the CA surfaces, and a fibrin network was clearly formed around the red blood cells. On the SOI surface, more red blood cells were observed, and a fibrin network was densely present above and around the red blood cells (Figure 5).

Platelet activation

The mean measurements of soluble P-selectin ELISA for the SA, CA, and SOI surfaces were 0.112, 0.251, and 0.414 OD, respectively (Table 4). The difference between the SA and CA surface groups was statistically significant (P=0.000). The differences between the SA and SOI surface groups and between the CA and SOI surface groups were also statistically significant (P=0.000 and P=0.000, respectively).

DISCUSSION

It was tested whether an SLA surface coated with a pH buffering solution displayed higher hydrophilicity and affinity for proteins, cells, and platelets than a conventional SLA surface. These *in vitro* studies conducted using several implant surfaces showed that this novel surface was superior to a conventional SLA surface.

Generally, wettability is quantified by the contact angle between a liquid drop and the solid surface of a flat disc. In this study, wetting velocity, which is the number of threads wetted by blood, was used to indirectly test wettability because the contact angles of the CA and

https://doi.org/10.5051/jpis.2019.49.6.366

SOI surfaces were almost 0°, making comparison between the groups using only the contact angle impossible. In fact, using wetting velocity to assess surface hydrophilicity or wettability may not yield accurate results. However, we still opted to measure wetting velocity because the ability to attract blood in clinical situations is what we ultimately wanted to assess. In some sense, this may be a methodological limitation of this experiment, because 2 surfaces with very high hydrophilicity were tested. The wetting velocity of the SA surface was almost 0, whereas it was much higher for the CA and SOI surfaces over a short period of time. Essentially, the SA surface appeared to be less hydrophilic than the other 2 surfaces because it was a dry surface that had not been in contact with any liquid, as used in clinical situations. For this reason, the superior result obtained for the SOI group may not have been due to the effect of the buffering agent itself. However, to compare the implant surfaces used in real clinical situations, it is reasonable to use a dry SLA surface rather than an SLA surface submerged in saline that is not isotonic. A previous study [10] comparing the SLA surface submerged in isotonic NaCl solution with a conventional SLA surface also used a dry surface for its control group.

The optimal degree of hydrophilicity of the implant surface remains unclear. Whether and if so, to what extent a super-hydrophilic implant surface is biologically and clinically superior to a conventional hydrophilic implant surface is not evident [9]. However, a more hydrophilic surface is thought to enhance osseointegration according to previous *in vivo* and human studies [8,10], as it yields higher bone-to-implant contact. Furthermore, surface wettability has been found to alter the biological responses of implant surfaces regarding the adhesion of proteins and other molecules, as well as cell interactions [9]. Similarly, in the present study, the SOI group with the highest wetting velocity also showed the highest affinity for proteins and osteoblasts.

The biochemical properties of implant surfaces, such as cell viability, cell proliferation, cell attachment, and differentiation, have been tested in previous *in vitro* studies [12-14]. Soares et al. [12] observed the biological performance of differently-treated implant surfaces. Cell viability (mitochondrial activity), cell attachment, serum total protein, and ALP were assessed. The characteristics of the implant surface can determine the cellular response around the implant, as well as the extent of proteins adsorbed on the surface.

Martin et al. [13] performed analyses of cell proliferation, DNA synthesis, ALP activity, RNA and protein synthesis, and proteoglycan synthesis using 5 types of implant surfaces and MG-63 osteoblast-like cells. Additionally, they observed the morphology and distribution of the cells cultured on each type of surface. Their study demonstrated that surface roughness could alter osteoblast proliferation, differentiation, and matrix production.

Eriksson et al. [14] investigated cell viability, ALP activity, the level of vascular endothelial growth factor, the presence of osteocalcin, and cells positive for bone morphogenetic protein-2 according to the surface energy of implant surfaces. Surface energy seemed to be particularly important at early stages, and high surface energy was shown to promote cell differentiation and activation.

In the present study, a proliferation assay was performed to assess the adhesion and proliferation of the MG-63 cells, which was visualized using the colorimetric method of formazan dye. SEM images showed that the cells on the SOI surfaces were more differentiated and had proliferated to a greater extent than those on the other surfaces.

https://doi.org/10.5051/jpis.2019.49.6.366

Osteoblast differentiation was represented by ALP concentration, since ALP is highly expressed in the proliferation stage of the osteoblast [21-24]. Osteoblast mineralization was represented by the quantification of calcified mineral stained with Alizarin Red S. Alizarin Red S binds to calcium deposits in cell cultures, which is useful for the detection of extracellular matrix calcification [27-29]. Additionally, osteoblast migration was tested with the Transwell® cell migration assay, which measures cell mobility toward a chemoattractant gradient [35]. Although the repeated number of experiments for cell adhesion, proliferation, differentiation, and mineralization was not statistically sufficient, there was a tendency for the SA surface to be the least osteoblast-friendly and the SOI surface to be the most osteoblast-friendly in this study.

Di Iorio et al. [16] observed fibrin clots on implant surfaces, and the black points on the SEM images, which were taken to indicate the presence of fibrin clots, were automatically counted using special software. In the present study, the platelet adhesion level was quantified by measuring LDH, which is released during the lysis of adherent platelets. The platelet activation level was quantified by measuring P-selectin, the platelet membrane glycoprotein expressed when platelets are activated. In the platelet adhesion test, the SOI surface showed the highest mean value, but without statistical significance compared to the CA surface. In the platelet activation test, the SOI surface exhibited the highest platelet activation, with statistical significance. The SEM images also showed the same results, with a network of red blood cells and fibrin clearly formed on the SOI surface.
Osteoblast activity peaks at pH 7.4, a weakly basic condition, and almost disappears below 6.9 [18,19]. In this experiment, a weakly basic medium was used to culture MG-63 cells, as in blood. Although the cell culture medium was exchanged periodically, the pH could not be kept constant, as it was impacted by the metabolites of the cells. Furthermore, various laboratory errors could affect pH in *in vitro* experiments. Even when drilling or destruction of bone does not occur, which would produce a weakly acidic pH, a pH buffer may be helpful to keep the pH constant even in *in vitro* conditions. The pH buffering agent seems to make conditions favorable for osteoblast activity by keeping pH constant or at least preventing significant changes in pH, as the results of this experiment showed increased osteoblast activity in the SOI group. Calcium ions also bind to various proteins in solution, keeping the solution pH weakly basic and functioning as a pH buffer. It should be taken into account that calcium ions themselves contribute to osteogenic processes, but it may also be important that the CA surface has a pH buffering effect, although it is not as effective as the SOI surface. In addition, platelet adhesion and activation were significantly higher on the CA and SOI surfaces than on the SA surface. Platelet activity is inhibited by extracellular acidosis and promoted by extracellular alkalosis [20]. Since platelet activity is affected by extracellular pH, it is thought that platelets may have been activated on the CA and SOI surfaces, which have a pH buffering effect.

In some experiments, significant differences were observed between the CA and SOI surfaces, whereas other experiments showed no significant differences. Since both CA and SOI surfaces have a pH-buffering effect in isotonic solution, the results of the experiments did not appear to be consistently different unless they showed a major effect on cell activity. In contrast, the SA surface, which was not immersed in solution and had no pH buffering effect, showed a significantly inferior results in most experiments.

An SLA surface with a pH buffering agent exhibited higher hydrophilicity and affinity for proteins, cells, and platelets than a conventional SLA surface. Since the number of

https://doi.org/10.5051/jpis.2019.49.6.366

experiments performed was not standardized and was statistically insufficient in some experiments, caution is needed in interpreting the results. Under acidic conditions after a drilling procedure, the pH buffering capacity is also expected to increase the level of ALP, promoting thrombogenesis and osteoblast activity. Within the limits of this study, it may be concluded that this novel surface can induce attachment to platelets, bone-forming proteins, and cells more than a conventional SLA surface, allowing stable and fast osseointegration to be achieved. Further studies should be conducted to directly compare an SLA surface with a pH buffering agent with other conventional surfaces with regard to its safety and effectiveness in clinical settings.

ACKNOWLEDGEMENTS

The authors would like to give special thanks to Osstem Implant Co., Ltd. for the technical support they provided in the conduction of this study.

REFERENCES

1. Massaro C, Rotolo P, De Riccardis F, Milella E, Napoli A, Wieland M, et al. Comparative investigation of the surface properties of commercial titanium dental implants. Part I: chemical composition. J Mater Sci Mater Med 2002;13:535-48.
PUBMED | CROSSREF
2. Albrektsson T, Wennerberg A. Oral implant surfaces: Part 2--review focusing on clinical knowledge of different surfaces. Int J Prosthodont 2004;17:544-64.
PUBMED
3. Esposito M, Coulthard P, Thomsen P, Worthington HV. The role of implant surface modifications, shape and material on the success of osseointegrated dental implants. A Cochrane systematic review. Eur J Prosthodont Restor Dent 2005;13:15-31.
PUBMED
4. Puleo DA, Thomas MV. Implant surfaces. Dent Clin North Am 2006;50:323-38, v.
PUBMED | CROSSREF
5. Le Guéhennec L, Soueidan A, Layrolle P, Amouriq Y. Surface treatments of titanium dental implants for rapid osseointegration. Dent Mater 2007;23:844-54.
PUBMED | CROSSREF
6. Morton D, Bornstein MM, Wittneben JG, Martin WC, Ruskin JD, Hart CN, et al. Early loading after 21 days of healing of nonsubmerged titanium implants with a chemically modified sandblasted and acid-etched surface: two-year results of a prospective two-center study. Clin Implant Dent Relat Res 2010;12:9-17.
PUBMED | CROSSREF
7. Li D, Ferguson SJ, Beutler T, Cochran DL, Sittig C, Hirt HP, et al. Biomechanical comparison of the sandblasted and acid-etched and the machined and acid-etched titanium surface for dental implants. J Biomed Mater Res 2002;60:325-32.
PUBMED | CROSSREF
8. Lang NP, Salvi GE, Huynh-Ba G, Ivanovski S, Donos N, Bosshardt DD. Early osseointegration to hydrophilic and hydrophobic implant surfaces in humans. Clin Oral Implants Res 2011;22:349-56.
PUBMED | CROSSREF
9. Gittens RA, Scheideler L, Rupp F, Hyzy SL, Geis-Gerstorfer J, Schwartz Z, et al. A review on the wettability of dental implant surfaces II: biological and clinical aspects. Acta Biomater 2014;10:2907-18.
PUBMED | CROSSREF
10. Buser D, Broggini N, Wieland M, Schenk RK, Denzer AJ, Cochran DL, et al. Enhanced bone apposition to a chemically modified SLA titanium surface. J Dent Res 2004;83:529-33.
PUBMED | CROSSREF
11. Scarano A, Piattelli A, Quaranta A, Lorusso F. Bone response to two dental implants with different sandblasted/acid-etched implant surfaces: a histological and histomorphometrical study in rabbits. BioMed Res Int 2017;2017:8724951.
PUBMED | CROSSREF

12. Soares PB, Moura CC, da Rocha Júnior HA, Dechichi P, Zanetta-Barbosa D. Biological characterization of implant surfaces - *in vitro* study. Rev Odontol UNESP 2015;44:195-9.
CROSSREF

13. Martin JY, Schwartz Z, Hummert TW, Schraub DM, Simpson J, Lankford J Jr, et al. Effect of titanium surface roughness on proliferation, differentiation, and protein synthesis of human osteoblast-like cells (MG63). J Biomed Mater Res 1995;29:389-401.
PUBMED | CROSSREF

14. Eriksson C, Nygren H, Ohlson K. Implantation of hydrophilic and hydrophobic titanium discs in rat tibia: cellular reactions on the surfaces during the first 3 weeks in bone. Biomaterials 2004;25:4759-66.
PUBMED | CROSSREF

15. Hong J, Kurt S, Thor A. A hydrophilic dental implant surface exhibits thrombogenic properties *in vitro*. Clin Implant Dent Relat Res 2013;15:105-12.
PUBMED | CROSSREF

16. Di Iorio D, Traini T, Degidi M, Caputi S, Neugebauer J, Piattelli A. Quantitative evaluation of the fibrin clot extension on different implant surfaces: an *in vitro* study. J Biomed Mater Res B Appl Biomater 2005;74:636-42.
PUBMED | CROSSREF

17. Kohn DH, Sarmadi M, Helman JI, Krebsbach PH. Effects of pH on human bone marrow stromal cells *in vitro*: implications for tissue engineering of bone. J Biomed Mater Res 2002;60:292-9.
PUBMED | CROSSREF

18. Arnett TR. Extracellular pH regulates bone cell function. J Nutr 2008;138:415S-8S.
PUBMED | CROSSREF

19. Kaysinger KK, Ramp WK. Extracellular pH modulates the activity of cultured human osteoblasts. J Cell Biochem 1998;68:83-9.
PUBMED | CROSSREF

20. Marumo M, Suehiro A, Kakishita E, Groschner K, Wakabayashi I. Extracellular pH affects platelet aggregation associated with modulation of store-operated Ca^{2+} entry. Thromb Res 2001;104:353-60.
PUBMED | CROSSREF

21. Engvall E. Enzyme immunoassay ELISA and EMIT. Methods Enzymol 1980;70:419-39.
PUBMED | CROSSREF

22. Jung K, Pergande M. Influence of inorganic phosphate on the activity determination of isoenzymes of alkaline phosphatase in various buffer systems. Clin Chim Acta 1980;102:215-9.
PUBMED | CROSSREF

23. Harada M, Hiraoka BY, Fukasawa K, Fukasawa KM. Purification and properties of bovine dental-pulp alkaline-phosphatase. Arch Oral Biol 1982;27:69-74.
PUBMED | CROSSREF

24. Jones JV, Mansour M, James H, Sadi D, Carr RI. A substrate amplification system for enzyme-linked immunoassays. II. Demonstration of its applicability for measuring anti-DNA antibodies. J Immunol Methods 1989;118:79-84.
PUBMED | CROSSREF

25. Rausch-fan X, Qu Z, Wieland M, Matejka M, Schedle A. Differentiation and cytokine synthesis of human alveolar osteoblasts compared to osteoblast-like cells (MG63) in response to titanium surfaces. Dent Mater 2008;24:102-10.
PUBMED | CROSSREF

26. Valarmathi MT, Yost MJ, Goodwin RL, Potts JD. The influence of proepicardial cells on the osteogenic potential of marrow stromal cells in a three-dimensional tubular scaffold. Biomaterials 2008;29:2203-16.
PUBMED | CROSSREF

27. Sudo H, Kodama HA, Amagai Y, Yamamoto S, Kasai S. *In vitro* differentiation and calcification in a new clonal osteogenic cell line derived from newborn mouse calvaria. J Cell Biol 1983;96:191-8.
PUBMED | CROSSREF

28. Gregory CA, Gunn WG, Peister A, Prockop DJ. An Alizarin red-based assay of mineralization by adherent cells in culture: comparison with cetylpyridinium chloride extraction. Anal Biochem 2004;329:77-84.
PUBMED | CROSSREF

29. Malladi P, Xu Y, Chiou M, Giaccia AJ, Longaker MT. Effect of reduced oxygen tension on chondrogenesis and osteogenesis in adipose-derived mesenchymal cells. Am J Physiol Cell Physiol 2006;290:C1139-46.
PUBMED | CROSSREF

30. Kanthan SR, Kavitha G, Addi S, Choon DS, Kamarul T. Platelet-rich plasma (PRP) enhances bone healing in non-united critical-sized defects: a preliminary study involving rabbit models. Injury 2011;42:782-9.
PUBMED | CROSSREF

31. Tamada Y, Kulik EA, Ikada Y. Simple method for platelet counting. Biomaterials 1995;16:259-61.
PUBMED | CROSSREF

32. Grunkemeier JM, Tsai WB, Horbett TA. Hemocompatibility of treated polystyrene substrates: contact activation, platelet adhesion, and procoagulant activity of adherent platelets. J Biomed Mater Res 1998;41:657-70.
PUBMED | CROSSREF

33. Park JY, Davies JE. Red blood cell and platelet interactions with titanium implant surfaces. Clin Oral Implants Res 2000;11:530-9.
PUBMED | CROSSREF

34. Klein MO, Grötz KA, Walter C, Wegener J, Wagner W, Al-Nawas B. Functional rehabilitation of mandibular continuity defects using autologous bone and dental implants - prognostic value of bone origin, radiation therapy and implant dimensions. Eur Surg Res 2009;43:269-75.
PUBMED | CROSSREF

35. Justus CR, Leffler N, Ruiz-Echevarria M, Yang LV. *In vitro* cell migration and invasion assays. J Vis Exp 2014:51046.
PUBMED | CROSSREF

https://doi.org/10.5051/jpis.2019.49.6.366